J Supercomput (2014) 69:1139–1153
DOI 10.1007/s11227-013-0964-1

Hybrid analog/digital wavelength-time optical CDMA systems in radio-over-fiber transmissions

Chih-Ta Yen · Hsu-Chih Cheng · Ing-Jr Ding

Published online: 7 June 2013

Abstract This study presents a hybrid analog/digital (A/D) mechanism of two-dimensional (2-D) structure of wavelength-hopping and time-spreading coding optical code-division multiple-access (OCDMA) system for future generation communication and network technologies. The 2-D method increases the maximum permissible number of simultaneous base stations (BSs) and security using a finite bandwidth of optical broad-band light source (BLS). In the proposed system, we can employ low-cost BLS which can mitigate the sampling rate of optical switch (OSW) and has the advantage of power saving. The performance enhancement is using the time-spreading method by a Mach-Zehnder modulator (MZM) with switch function to suppress the phase-induced intensity noise (PIIN) effect of the wavelength domain and the receiver structure is equipped with balanced detectors in order to suppress the multiple-access interference (MAI). In addition, the hybrid OCDMA network is equipped using a dual input MZM for the choice which time analog or digital signals to be transmitted and the advantage of these two kinds of signals can transmit by the same coder/decoder (codec) mechanism and recover by different type filters in the receiver end. The numerical evaluation results demonstrate that, for analog and digital signals under PIIN- and MAI-limited conditions, the proposed system outperforms a conventional multi-wavelength and time-spreading OCDMA scheme. Hence, enhancing the confidentiality of the asynchronous networks of codeword assignments and integratable hardware designs for the scheme with a MZM, an optical switch (OSW), arrayed-waveguide grating (AWG) and fiber Bragg gratings (FBGs) in hybrid A/D 2-D OCDMA system is proposed.

C.-T. Yen · I.-J. Ding (✉)
Department of Electrical Engineering, National Formosa University, Yunlin, Taiwan
e-mail: eugen.ding@gmail.com

H.-C. Cheng
Department of Electro-Optics Engineering, National Formosa University, Yunlin, Taiwan

Keywords Optical code-division multiple-access (OCDMA) · Two-dimensional (2-D) · Optical switch (OSW) · Phase-induced intensity noise (PIIN) · Multiple-access interference (MAI)

1 Introduction

Recently, the green issue has come to the picture seeking immediate solutions for communication systems to be energy-efficient and environmentally protected. Optical fiber micro-cellular systems, in which micro-cells distributed over a wide geographic area are connected by optical fibers, and radio signals are transmitted over these optical fiber links between the base stations (BSs) and the central station (CS), have attracted considerable attention. These architectures enable an effective increase in the available bandwidth, thus increasing the maximum permissible number of simultaneous BSs and supporting the provision of broad-band services such as cloud computing technology, and they have the advantage of power saving.

The process of modulating RF signals onto an optical carrier for distribution over a fiber network is referred to as "radio-over-fiber (RoF)" [1–5]. RoF links are designed to transfer radio signals to remote stations without losing their original radio format, e.g., their frequencies, modulation formats, and so on. RoF technology has a number of key advantages, including a low cost and the ability to perform RF allocation of channels with various modulated formats at a CS, thus permitting a flexible allocation process and a rapid response to variations in the traffic demand [6–8].

A typical BS consists of an electro-optical (E-O) modulator to receive the RF signal and to send it to the CS and an optical-electro (O-E) demodulator to receive signals from the CS and to transmit the corresponding RF signal. In other words, the BS has only two functions, namely to transmit RF signals to the CS in an optical format and to transmit RF signals in an electrical format. More complex tasks such as modulating the RF signal to an appropriate format are performed at the CS as shown in Fig. 1.

Following the successful application of code-division multiple-access (CDMA) techniques in wireless communications, many researchers have investigated the feasibility of optical CDMA (OCDMA) systems. OCDMA provides a powerful solution for RoF network access schemes designed to allow multiple users to access the same fiber channel in local area networks (LANs) asynchronously without delay or the need for scheduling.

In the study, we perform time-domain multiplexing by time-spreading optical pulses of Mach-Zehnder modulator (MZM) modulator with the same function as optical switches (OSWs) and called direct optical switching (DOS)-CDMA [4, 5]. In DOS-CDMA method, if the sampling rate of OSW is not fast enough and therefore multiple-access interference (MAI) is increased and hence it destroys system performance.

Two-dimensional (2-D) codes are developed to overcome the long length of one-dimensional (1-D) optical codes to suppress the MAI problem. But there are few papers discussing RF analog links in 2-D OCDMA schemes. For example, one kind of 2-D optical codes is to apply the maturely developed 1-D codes in combined time-spreading and wavelength-hopping scheme. In such a system, the concept of the 2-D

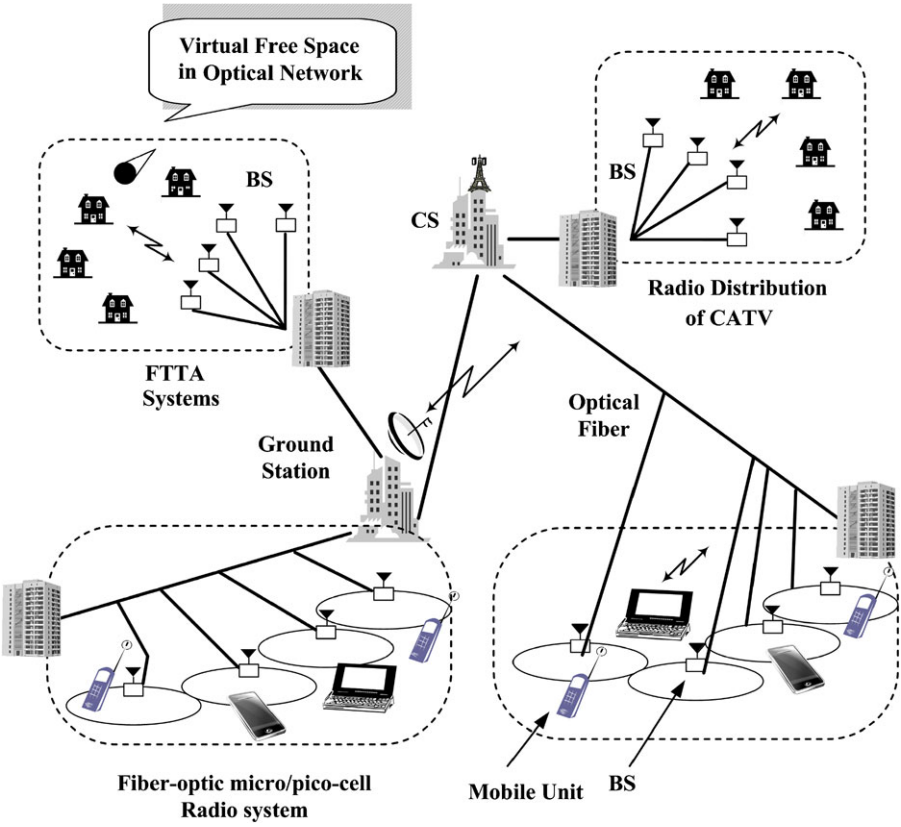

Fig. 1 Concept of RoF network

coding scheme was first to spread a broad-band short laser pulse into pulses of different wavelengths by using a wavelength-demultiplexing device. Second, it performs coding by controlling the amplitudes and time delays of these pulses. Finally, the coded pulses recombine by a wavelength-multiplexing device [9–11]. These methods can be applied for optical digital modulation; however, it is difficult to apply them for multiplexing radio signals for analog links. The other kinds of method are to use spatial-frequency for 2-D OCDMA [12, 13], however, the power unmatched problem becomes more serious when the system is not in synchronization. And then the technique of 2-D wavelength-time (W-T) OCDMA [14] is proposed by using OSWs and arrayed-waveguide gratings (AWGs), but the decoder mechanism has more complexity to apply in hybrid analog/digital (A/D) systems.

The proposed 2-D OCDMA system uses low in-phase cross correlation of prime codes as time-spreading code and multi-weight of M-sequence code as wavelength-hopping code. High power efficiency and low-cost BLS are employed for our hybrid system, such as high power LED. We use MZM to perform a time-spreading method to suppress the noise of PIIN [14–16] in multi-wavelength system. We have fiber Bragg gratings (FBGs) equipped balanced photo-detectors (PDs) to perform the

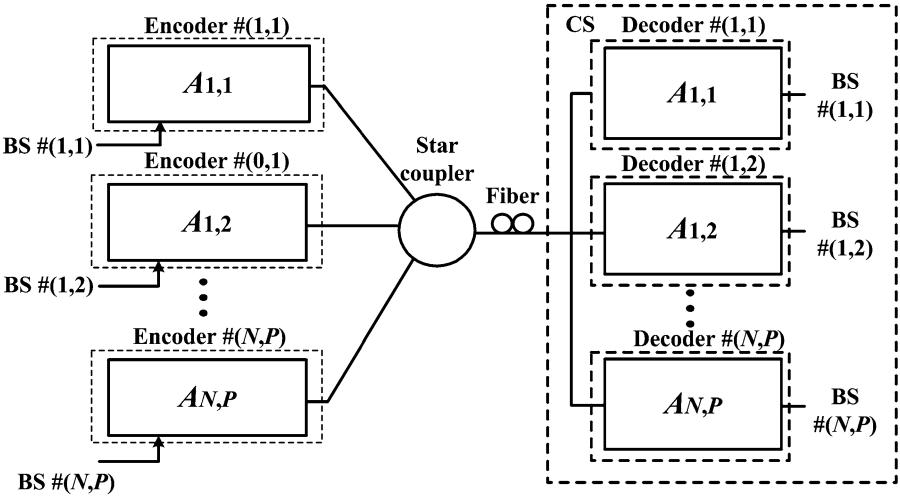

Fig. 2 Integrated configuration of hybrid A/D 2-D OCDMA system

wavelength-hopping technique to suppress MAI in a time-coded system. Therefore, conventional low-cost broad-band light sources and compact optical components are sufficient for hybrid coder/decoders to transmit A/D signals and its implementation, rendering the overall system both cheap and straightforward. The remainder of this paper is organized as follows. Section 2 provides an overview of the W-T code construction and the system configuration. Section 3 evaluates the system performance and discusses the dominated noise effects. Finally, Sect. 4 presents some brief conclusions.

2 System description

Figure 2 shows the integrated diagram of the proposed 2-D OCDMA system. A family of prime code with ideal cross correlation has been proposed for each prime number P. This prime code is constructed based on GF(P) with its code length P^2 to use in the time-spreading code. N is the code length of the M-sequence code, there are N M-sequence code sequences with auto-correlation $N + 1/2$ and cross-correlation function $N + 1/4$ to use in the wavelength-hopping code. Every BS is assigned with one W-T matrices codeword $A_{k,l}, k = 1, \ldots, N$ and $l = 1, \ldots, P$.

Let $\boldsymbol{X}_k = [x_k(1), x_k(2), \ldots, x_k(N)]$ and $\boldsymbol{Y}_l = [y_l(1), y_l(2), \ldots, y_l(P)]$ be two unipolar sequences. $\boldsymbol{X}_k$ and $\boldsymbol{Y}_l$ are the M-sequence codes and prime codes of length N and P^2, respectively. The elements of the 2-D Matrix $\boldsymbol{A}_{k,l}$ for BS #(k, l) is obtained as follows:

$$\boldsymbol{A}_{k,l} = \boldsymbol{X}_k^T \boldsymbol{Y}_l = \begin{bmatrix} x_1 y_1 & x_1 y_2 & \cdots & x_1 y_P \\ x_2 y_1 & x_2 y_2 & \cdots & x_2 y_P \\ \vdots & \vdots & \cdots & \vdots \\ x_N y_1 & x_{N-1} y_2 & \cdots & x_N y_P \end{bmatrix}. \quad (1)$$

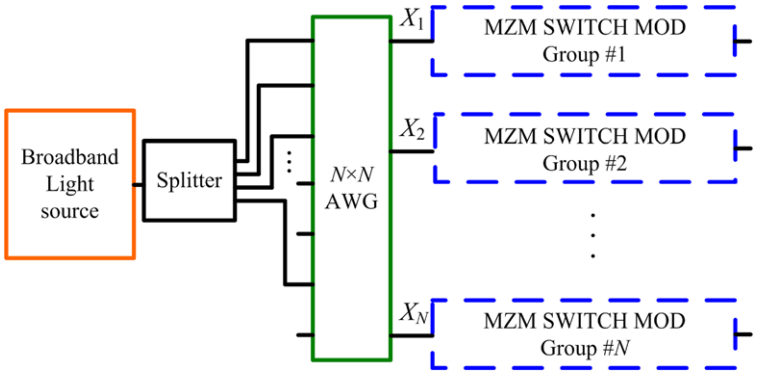

Fig. 3 Wavelength-time encoder of hybrid A/D 2-D OCDMA system

The binary bits of each BS are encoded with the corresponding 2-D codewords by the proposed 2-D encoder. All coded radio signals are combined in the star couplers and broadcast to the CS of each decoder. The CS decoder uses a 2-D decoder to extract the RF signal according to the BS.

In analog transmission, the radio signal $g_{k,l}(t)$ at the transmitter has the form

$$g_{k,l}(t) = a_{k,l}(t)\cos(2\pi f_{rf} t). \tag{2}$$

Here f_{rf} is the carrier frequency of the radio signal and $a_{k,l}(t)$ is the complex envelope with a bandwidth B_{rf}. As discussed above, in the proposed 2-D OCDMA scheme, an optical ON-OFF switching function is performed using a dual input MZM-based switch driven by the unipolar prime-sequence code $y_l(t)$. Since the pulse amplitude is either one or zero, the intensity of the optical pulse amplitude modulation/IM (PAM/IM) signal at the output of the MZM is given by

$$P_{k,l}(t) = P_S\big[1 + g_{k,l}(t)\big]y_l(t), \tag{3}$$

where P_S is the average transmitted optical power of the broad-band light source prior to optical switching.

In Eq. (3), $P_{k,l}$ is a bandpass natural sampled signal [17, 18] converted from a radio signal by an optical switching process performed using window-type sampling with a sampling period of less than or equal to half of the inverse of the radio signal bandwidth ($Rs \geqq 2B_{rf}$). In implementing the present 2-D OCDMA scheme, this study considers the case of a synchronous signal transmission. When the digital data is transmitted, the radio signal $g_{k,l}$ is instead of low frequency of rectangular pulse. And Eq. (3) becomes the unit amplitude constant value during one bit period.

As shown in Fig. 3, the proposed 2-D OCDMA transmitter consists of an MZM SWITCH MOD groups connecting by wavelength encoder and then sends the radio signal to star coupler. In the transmitter of the proposed system, MZMs and the common AWG router are assigned to each BS to implement the 2-D A/D schemes, respectively. The wavelength encoded operation mechanism is similar to reference [14]. Figure 3 shows the general case where the AWG router-based wavelength encoder in the transmitter is used to encode the radio signals of MZM SWITCH MOD groups.

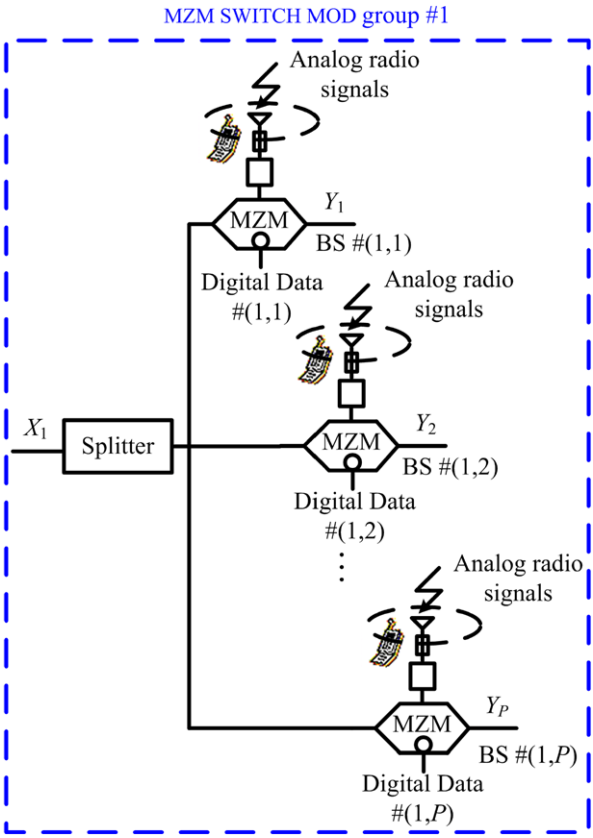

Fig. 4 Hybrid A/D time-spreading encoder group #1

The wavelength of the broad-band light source incident at the input ports of the AWG router is demultiplexed into wavelengths $\lambda_1 \sim \lambda_N$ and these wavelengths are distributed across the output ports of the router as a result of interference in the second slab of the waveguide. The signals of the same wavelength incident at different input ports are directed to different output ports by cyclic properties [14]. Let $\boldsymbol{X}_1 = (x_{1,1}, x_{1,2}, \ldots, x_{1,N})$ be a unipolar M-sequence codeword of length N assigned as the codeword of OSW MOD group #1. The codeword of the ath wavelength's sequence ($a = 1, \ldots, N$) can be obtained by cyclically shifting the original sequence (i.e., $\boldsymbol{X} = T^a \boldsymbol{X}_1$). In this arrangement, the AWG router input ports corresponding to a wavelength pattern of unipolar M-sequence code element of "1" are connected to the broad-band light source.

As shown in Fig. 4, the MZM SWITCH MOD group consists of a splitter, a dual input port of MZM modulator with switch function which can transmit either digital or analog signals, and performs the switch function of the time-spreading method. Initially, the radio signal of BS #(k, l) is converted into a coded spectrum signal by AWG encoder. The spectral code $\boldsymbol{X}_k$ is then sampled at an MZM, which is driven with a specified time-spreading code sequence $\boldsymbol{Y}_l$. The output signals of the MZM are transmitted to an optical copular. The resultant W-T code, $\boldsymbol{A}_{k,l}$, is then passed to the star coupler.

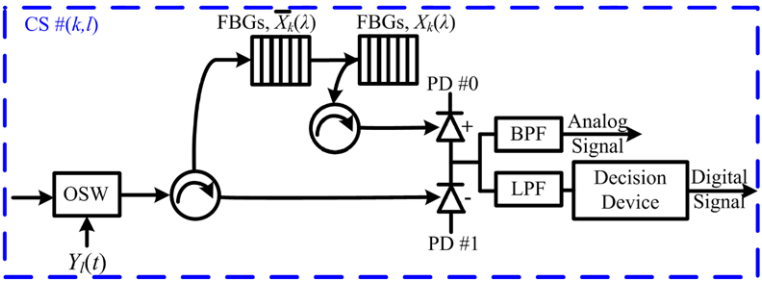

Fig. 5 Wavelength-time decoder of hybrid A/D 2-D OCDMA system

In order to gain the largest code length at the same switching speed of the OSW; the chip width T_C is given by T_F/P^2. Spectral encoding is accomplished using a single AWG demultiplexer connected to the output of the MZM-based switch MOD. The corresponding switch signal of ith AWG output port remains "ON" for as long as ith chip of the spectral codeword is "1". Under these conditions, when the radio signal is sampled by the MZM switch, the ith wavelength from the MZM switch-sampled signal is transmitted to the star coupler. Conversely, when the ith chip of the spectral codeword is "0", the link between the AWG output port and the optical combiner is "OFF", corresponding to the transmission of all-zero spectral chips. Thus, the beating terms at the PD will be suppressed.

The W-T OCDMA decoder is shown in Fig. 5. The star coupler is connected to the decoder's OSW driven with a time-spreading code sequence, $\boldsymbol{Y}_l$. The OSW is connected to the spectral decoder of FBGs, which distributes received signals to the balanced PD of each time-spreading decoder group to realize differential decoding. The connections from the FBGs to the upper and lower optical couplers are determined by the $\boldsymbol{X}_k$ codeword and its complementary codeword $\overline{\boldsymbol{X}}_k$, respectively. The balanced PD of spectral decoder #k will receive $\boldsymbol{Y}_l\boldsymbol{X}_k$ from the upper arm and $\boldsymbol{Y}_l\overline{\boldsymbol{X}}_k$ from the lower arm. After correlation subtraction $\boldsymbol{Y}_l\boldsymbol{X}_k - \boldsymbol{Y}_l\overline{\boldsymbol{X}}_k$ is performed in the kth wavelength-hopping decoder's balanced PD, the sampled optical signal of time-spreading decoder #l is subsequently recovered and other wavelength-hopping decoder groups' interferences are rejected.

We use a time sampled and spectral balanced detector structure that can suppress dominant noises of MAI and spectral PIIN that co-exist. As discussed later, this structure successfully suppresses both the PIIN beat noise and the MAI effect.

The study presents the concepts of correlation-decoding scheme to MAI-suppression for 2-D matrix coding. Assume that BS #(k, l) is the desired signal. The elements of the two decoding matrices $A^{(d)}$ $(d = 0, 1)$ are defined as

$$a_{k,l}^{(0)}(i, j) = X_k(i)Y_l(j), \qquad a_{k,l}^{(1)}(i, j) = \overline{X}_k(i)Y_l(j). \tag{4}$$

After passing through the time decoder and the wavelength decoder in both arms, the original signal, which contains not only the codeword representing the desired signal, but also an interference component, is separated into two parts. Hence, correlation subtractions $\sum_{b_{p,q}=1}^{p,q} [R_{AA}^{(0)}(k, l, p, q)]$ in the upper arm and $\sum_{b_{p,q}=1}^{p,q} [R_{AA}^{(1)}(k, l, p, q)]$ in the lower branch can be effectively implemented. The

receivers which compute the correlation subtractions $[R_{AA}^{(0)}(k,l,p,q)] - [R_{AA}^{(1)}(k,l,p,q)]$ suppress the interference arising from BS $\#(p,q)$, which is assigned an 2-D matrix codeword of $A_{p,q}$. The correlation subtraction process suppresses MAI in the decoder output and enables the desired radio signal to be extracted.

The corresponding correlation functions with respect to the interfering codeword $A_{p,q}$ of BS $\#(p,q)$ are:

$$R_{AA}^{(d)}(k,l,p,q) = \sum_{i=0}^{N-1}\sum_{j=0}^{L-1} a_{k,l}^{(d)}(i,j)a_{p,q}(i,j) = \begin{cases} (\frac{N+1}{2})p, & \text{for } k=p, l=q \\ (\frac{N+1}{2}), & \text{for } k=p, l\neq q \\ 0, & \text{otherwise.} \end{cases} \tag{5}$$

Four circumstances are relevant in the receiver: (1) the same wavelength-hopping patterns and the same time-spreading patterns; (2) the same wavelength-hopping patterns and a different time-spreading patterns; (3) different wavelength-hopping patterns and the same time-spreading patterns; and (4) different wavelength-hopping patterns and different time-spreading patterns. Case 1 is the desired signal in the system. Case 2 will lead to the MAI problem. However, the MAI will be low compared with that of the desired signal component when the length of the time-spreading code is long. In Cases 3 and 4, the proposed 2-D scheme will effectively cancel out MAI.

3 Performance analysis and discussion

The performance of the proposed 2-D OCDMA system is mainly limited by PIIN and MAI effects, particularly when the received power is high. PIIN results from the beating of incoherent light fields during the direct detection of square-law PDs and its magnitude depends essentially on the state of polarizations (SOPs) and spectra of the optical signals. For analyzing the effects of PIIN and MAI, the study calculates the carrier to noise power ratio due to the effect of PIIN ($\mathrm{CNR_{PIIN}}$) and carrier to interference power ratio ($\mathrm{CIR_{MAI}}$), respectively. Finally, the discussion of all noises plus interference effects in the proposed 2-D OCDMA-based RoF system is presented. To simplify the current system performance analysis, the analysis assumptions are made as in [14].

After the encoding process, the coded spectra of $\boldsymbol{S}_{k,l}$ represent the optical carriers used to transmit the MZM switch-sampled optical signal for BS $\#(k,l)$. The spread optical signals from each BS are combined by the star coupler and sent to the receiver. The spectrum, $\boldsymbol{S}$, of the received signal is therefore comprised of all the transmission signal spectra of the individual BS in the network, i.e.

$$\begin{aligned} S(\nu,t) &= (s_{1,1}, s_{1,2}, \ldots, s_{2,1}, \ldots, s_{M,D}) \\ &= \frac{P_{sr}}{\Delta\nu}\sum_{m=1}^{M}\sum_{d=1}^{D}\sum_{i=1}^{N}\big[1+g_{m,d}(t)\big]x_m(i)\,y_d(t)\big\{\Pi(i)\big\}. \end{aligned} \tag{6}$$

where

$$\Pi(i) = u\left[\nu - \nu_0 - \frac{\Delta\nu}{2N}(-N+2i-2)\right] - u\left[\nu - \nu_0 - \frac{\Delta\nu}{2N}(-N+2i)\right] \tag{7}$$

and $u(\nu)$ is the unit step function, P_{sr} is the effective source power from a single source at the receiver, D is the number of BS using time-spreading patterns, and M is the number of BS using wavelength-hopping patterns.

The instantaneous PSDs of the light incident at PD #0 and PD #1 of the receiver for the codeword $\boldsymbol{A}_{k,l}$ during one bit period can be written as

$$G_0(\nu,t) = \frac{P_{sr}}{\Delta\nu}\sum_{m=1}^{M}\sum_{d=1}^{D}\sum_{i=1}^{N}\big[1+g_{m,d}(t)\big]x_m(i)y_d(t) \cdot \big[x_k(i)y_l(t)\big]\big\{\Pi(i)\big\} \tag{8}$$

and

$$G_1(\nu,t) = \frac{P_{sr}}{\Delta\nu}\sum_{m=1}^{M}\sum_{d=1}^{D}\sum_{i=1}^{N}\big[1+g_{m,d}(t)\big]x_m(i)y_d(t) \cdot \big[\overline{x_k}(i)y_l(t)\big]\big\{\Pi(i)\big\}. \tag{9}$$

The input current to the bandpass filter (BPF) and lowpass filter (LPF) can be written as

$$\begin{aligned} i_o(t) &= i_0(t) - i_1(t) \\ &= i_{S_{k,l}}(t) + i_{\mathrm{MAI}}(t) + i_{\mathrm{PIIN}}(t) + i_{\mathrm{shot}}(t) + i_{\mathrm{thermal}}(t), \end{aligned} \tag{10}$$

where $i_{S_{k,l}}(t)$, $i_{\mathrm{MAI}}(t)$, $i_{\mathrm{PIIN}}(t)$, $i_{\mathrm{shot}}(t)$, and $i_{\mathrm{thermal}}(t)$ are the desired radio signal, the interference, the PIIN noise, the shot noise, and the thermal noise, respectively.

The terms of $i_{S_{k,l}}(t)$ and $i_{S_{k,l}}(t)$ are expressed as

$$i_{S_{k,l}}(t) = i_0(t) - i_1(t) = \frac{RP_{sr}}{2}g_{k,l}(t)y_l(t), \tag{11}$$

$$i_{\mathrm{MAI}}(t) = \frac{RP_{sr}}{2}\sum_{\substack{e=1\\ e\neq l}}^{E} g_{k,e}(t)s_e(t)\big[2y_l(t)-1\big], \tag{12}$$

where R is the responsivity of PD.

The variation of the photocurrent caused as a result of PIIN is given by

$$\big\langle I_{\mathrm{PIIN}}^2\big\rangle = E\big[I^2\big(1+O^2\big)B\tau_{\mathrm{c}}\big], \tag{13}$$

where E is the expectation operator, I is the average photocurrent, B is the noise-equivalent electrical bandwidth of the receiver, and τ_c is the coherence time of the source, expressed as

$$\tau_{\mathrm{c}} = E\left\{\frac{\int_0^\infty G^2(\nu,t)\,d\nu}{[\int_0^\infty G(\nu,t)\,d\nu]^2}\right\}. \tag{14}$$

Table 1 Average variance of the cross-correlation of the prime codes

P	σ_C^2
7	0.272
11	0.298
13	0.303
23	0.318
31	0.322
47	0.326
71	0.328
97	0.329

and the degree of polarization (DOP), O, is defined as

$$O^2 = \frac{(\langle s_1 \rangle^2 + \langle s_2 \rangle^2 + \langle s_3 \rangle^2)}{\langle s_0 \rangle^2}, \tag{15}$$

where s_0, s_1, s_2, and s_3 are Stokes parameters used to express the SOP. The bracket $\langle\rangle$ in Eq. (15) denotes the average value of the parameter over wavelength, time, or space. It is well known that the DOP is dependent on not only the light source, but also the distance traveled by the optical signal in long-haul network transmissions. In Eq. (14), $G(\nu, t)$ is assumed to be the single sideband instantaneous PSD of the source.

Since the noises at the upper and lower PDs are independent, the power of the noise sources in the output photocurrent can be written as

$$\langle I_{\text{PIIN}}^2 \rangle = \frac{BRP_{sr}^2}{N\Delta\nu} \left\{ (1 + O^2) \left(\frac{N+1}{4} \right) \frac{K}{P} \left(\frac{K}{P} + 1 \right) \right\}. \tag{16}$$

The CNR due to the effect of PIIN is

$$\text{CNR}_{\text{PIIN}} = \frac{(N+1)P\Delta\nu}{BN(1+O^2)(K/P)(K/P-1)}, \tag{17}$$

where $\Delta\nu = 6.25$ THz (i.e. the common bandwidth of the light source is equivalent to 50 nm with a central wavelength of 1550 nm), $B = 80$ MHz, P is the code length of the prime code, and K is the number of simultaneous active BSs. To imply our 2-D system in the time domain, a code sequence with the highest possible auto-correlation and the lowest possible cross-correlation needs to be chosen. Therefore, the prime code sequence that can provide the highest auto-correlation and lowest cross-correlation is employed as a spread-spectrum (SS) code. Then, the CIR can be expressed as

$$\text{CIR}_{\text{MAI}} = \frac{PN}{\sigma_C^2(K-N)}, \tag{18}$$

where σ_C^2 denotes the average variance of the cross-correlation of the prime codes, and N is the code length of the M-sequence codes. Table 1 shows that σ_C^2 has a little increased as P increases but it will saturate at 0.329 for $P = 97$.

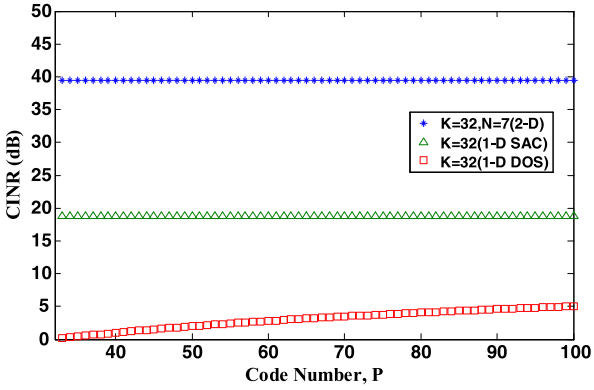

Fig. 6 CINR versus code sequence number at number of BS = 32

The shot noise power can be calculated according to Eq. (2) for *eIB* and is expressed as

$$\langle i_{\text{shot}}^2 \rangle = eBRP_{sr}\frac{K}{P}, \tag{19}$$

where e is the electron's charge.

The thermal noise power can be written as

$$\langle i_{\text{thermal}}^2 \rangle = \frac{4K_bT_nB}{R_L}, \tag{20}$$

where K_b is Boltzmann's constant, T_n is the absolute receiver noise temperature, and R_L is the receiver load resistor.

The system performance of carrier-to-interference-plus-noise ratio (CINR) performance of the regenerated signal can be obtained by combining Eqs. (17), (18), (19), and (20), i.e.,

$$\text{CINR} = \frac{\langle i_{s_{k,l}} \rangle}{\langle i_{\text{MAI}}^2 \rangle + \langle i_{\text{PIIN}}^2 \rangle + \langle i_{\text{shot}}^2 \rangle + \langle i_{\text{thermal}}^2 \rangle}. \tag{21}$$

Figure 6 illustrates the variation of the CINR with the time-spreading code sequence length, P. Note that the calculations are performed using the following parameters: $R = 0$, and the length of wavelength-hopping code is 16. In conventional spectral-amplitude-coding (SAC) OCDMA systems [15, 16], the CINR cannot be improved by increasing the code sequence length since this causes the beating of the wavelengths to become more severe and hence degrades the system performance. The MAI becomes the dominant noise of the DOS-CDMA scheme especially in the case of short code length. However, as the length of codes increases, the processing gain in the DOS scheme increases markedly to suppress the dominant MAI and therefore the CINR performance is improved at large number of BSs. However, if we increase the code length of the time-spreading code, this can suppress the beating terms as a result of the increased processing gain in the proposed 2-D OCDMA system. The CINR of the proposed scheme is significantly better than that of the conventional SAC and DOS-OCDMA schemes below 20 dB and 36 dB in the conditions that the number of code sequence is 63 and the number of active BSs is 32.

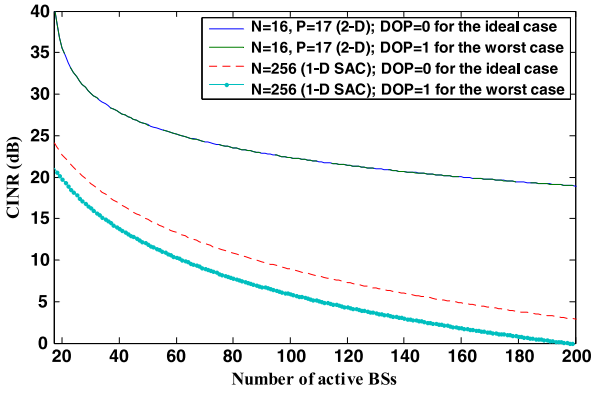

Fig. 7 CINR performance with degree of polarization, DOP

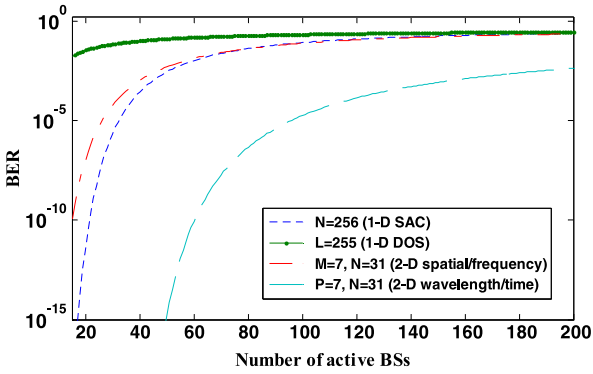

Fig. 8 BER versus number of simultaneous active BSs in analog scenario

A common un-polarized amplified spontaneous emission (ASE) source can be used in the current 2-D OCDMA system because the scheme considers only the source power, but not phase or polarization properties. However, on the long-haul transmissions over FTTX network and some polarized elements are used, the DOP effect must be addressed. In the study, we discusses the relationship between the CINR performance and the variations of the DOP (i.e., the DOP varies in the range 0 to 1) to represent the influence of polarization following long-haul transmission.

The CINR performance of the proposed 2-D OCDMA scheme is characterized by an upper bound of $R = 1$ for the worst case and a lower bound of $R = 0$ for the ideal case with the same assumption of $N = 16$ and $P = 17$ as shown in Fig. 7. Obviously, in the ideal case, by placing a scrambler in front of the balanced PD to cancel the polarization effect (i.e., $R = 0$), the performance of the 1-D SAC-OCDMA can be enhanced. Compared to the average DOP of 1 for the worst case, the CINR of the proposed 2-D scheme is improved about 16.5 dB when the number of BS is 100. By combining the time-spreading method with the wavelength-hopping scheme, the proposed 2-D system is insensitive of polarization states in the transmission links.

By assuming all the interference terms to be Gaussian distributed, the conditional bit error rate (BER) can be calculated from digital communication of amplitude shift keying (ASK) modulation, i.e., on employing $\mathrm{BER} = 0.5\mathrm{erfc}(\sqrt{\mathrm{CINR}/8})$, we can obtain the relation BER and the number of simultaneous active BSs as a function of

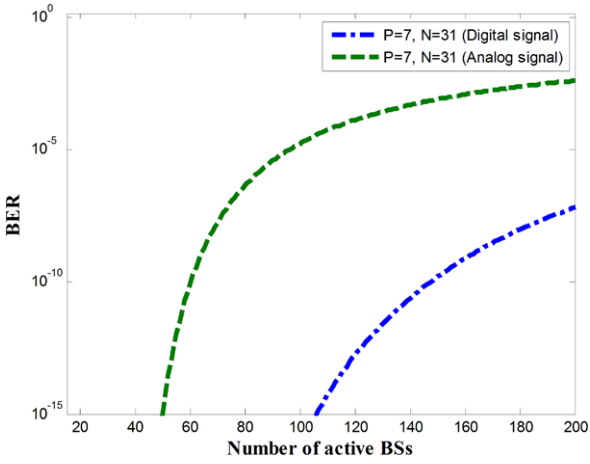

Fig. 9 BER versus number of simultaneous active BSs in analog and digital scenarios

the length. Figure 8 plots the variation of the BER with the number of active BSs as a function of the length of several codes. It can be seen that the BER of the conventional DOS system is worse than that of the SAC and proposed 2-D OCDMA systems, particularly when we have a small number of BSs. The MAI effect becomes dominant noise at short code length. However, in the spectral-coded OCDMA system, when a large number of BSs transmit their coding patterns simultaneously, more wavelengths beat together during the direct detection by the square-law PDs, the PIIN becomes the dominant noise degrading BER performance. Besides, the performance for the SAC-OCDMA system cannot be improved by increasing code length. The 2-D spatial/frequency OCDMA system [12, 13] suffers a serious power loss problem due to more optical couplers being used in the system and more insertion losses occur especially at small number of BSs. In general, the time-spreading method of DOS-CDMA performance can be enhanced by increasing code length i.e., increasing processing gain, but the code length must be very long to maintain high system performance. The DOS method needs high sampling rate of OSW to support long code length and makes the system impractical. In the proposed 2-D OCDMA scheme, the tradeoff on code length between time-spreading and wavelength-hopping codes can be considered in different RoF links; hence the system flexibility is increased.

Figure 9 shows the difference performance between the digital and analog transmissions with the same assumptions of Fig. 8. We can find that the digital signal is better than analog signal; this is because the threshold device is only needed to distinguish which data format of zero or one is transmitted in digital transmissions. But the phase and amplitude conditions should be considered in an analog link and hence a worse performance is obtained. The digital signal can support more than 100 BSs compared to an analog signal when the BER is 10^{-9}.

4 Conclusion

Novel design of hybrid A/D 2-D OCDMA-based RoF system with optical elements of dual input MZM, OSW, AWG, and FBGs is proposed. The system is designed

to increase the utilization of a broad-band light source with a finite bandwidth and release the sampling rate of OSW in the traditional OCDMA RoF system. In the proposed system, the number of encoder/decoder pairs and the required code length are more flexibility compared to conventional 2-D OCDMA systems. Furthermore, with the proposed system design, switched intensity modulators work with broad-band light source can be accomplished via one AWG router in the transmitter, thus wavelength mismatch between network coders can be avoided. The evaluation results have demonstrated that both PIIN can be suppressed in theory by avoiding the wavelengths beating at the same time and MAI can be canceled out by transmitting the RF signals of the BSs from different wavelength-hopping patterns in the system and hence increases the system performance. The BER of the hybrid A/D 2-D OCDMA system has been analyzed numerically for the PIIN and MAI limited case plus with shot and thermal noises. As the time-spreading prime code length is increased, the PIIN and MAI which suppress are increased relative to the processing gain and hence the noise suppression effect is effective. Besides, we can find that the BER performance of digital data is better than analog RF signal in the same system architecture. The flexible implementation of codewords assignments and integratable hardware designs for the scheme with optical integration elements of dual MZM switch, optical switch, and optical filters is proposed.

References

1. Way WI (1993) Optical fiber based microcellular systems: an overview. IEICE Trans Commun E 76-B(9):1091–1101
2. Wu JS, Wu J, Tsao HW (1998) A radio-over-fiber network for microcellular system application. IEEE Trans Veh Technol 47(1):84–94
3. Al-Raweshidy H, Komaki S (2002) Radio over fiber technologies for mobile communication networks. Artech House, Boston
4. Tsukamoto K, Higashino T, Nakanishi T, Komaki S (2003) Direct optical switching code-division multiple-access system for fiber-optic radio highway networks. IEEE/OSA J Lightwave Technol 21(12):3209–3220
5. Park S, Tsukamoto K, Komaki S (1998) Polarity-reversing type photonic receiving scheme for optical CDMA signal in radio highway. IEICE Trans Electron E 81-C(3):462–467
6. Hongli L, Shyu M-L (2011) Quality of service provision in mobile multimedia—a survey. Hum-Cent Comput Inf Sci 1(5):1–15
7. Hua Ho A, Ho YH, Hua KA, Villafane R, Chao H-C (2010) An efficient broadcast technique for vehicular networks. J Inf Process Syst 7(2):221–240
8. Pinaki S, Amrita S (2011) Security enhanced communication in wireless sensor networks using Reed-Muller codes and partially balanced incomplete block designs. J Converg 2(1):23–30
9. Kwong WC, Yang GC, Chang CY (2005) Wavelength-hopping time-spreading optical CDMA with bipolar codes. IEEE/OSA J Lightwave Technol 23(1):260–267
10. Yu K, Shin J, Park N (2000) Wavelength-time spreading optical CDMA system using wavelength multiplexers and mirrored fiber delay lines. IEEE Photonics Technol Lett 12(9):1278–1280
11. Wang Z, Chang J, Prucnal PR (2002) Theoretical analysis and experimental investigation on the confidentiality of 2-d incoherent optical CDMA system. IEEE/OSA J Lightwave Technol 28(12):1761–1769
12. Yang CC, Huang JF (2003) Two-dimensional M-matrices coding in spatial/frequency optical CDMA networks. IEEE Photonics Technol Lett 15(1):168–170
13. Yeh B-C, Lin C-H, Wu J (2010) Noncoherent spectral/spatial OCDMA system using two-dimensional hybrid codes. IEEE/OSA J Opt Commun Netw 2(9):653–661
14. Yen C-T, Huang J-F (2009) Realization of OSW/AWG-based bipolar wavelength-time optical CDMA for wired-wireless transmissions. Opt Fiber Technol 15(1):74–82

15. Smith EDJ, Blaikie RJ, Taylor DP (1998) Performance enhancement of spectral-amplitude-coding optical CDMA using pulse-position modulation. IEEE Trans Commun 46(9):1176–1185
16. Wei Z, Shalaby HMH, Ghafouri-Shiraz H (2001) Modified quadratic congruence codes for fiber bragg-grating-based spectral-amplitude-coding optical CDMA systems. IEEE/OSA J Lightwave Technol 19(9):1274–1281
17. Harada H, Kajiya S, Tsukamoto K, Komaki S (1995) TDM intercell connection fiber-optic bus link for personal radio communication systems. IEICE Trans Commun E 78-B(9):1287–1294
18. Kohlenberg A (1953) Exact interpolation of band-limited functions. J Appl Phys 12(12):1432–1436